Transp Porous Med (2015) 107:153–170
DOI 10.1007/s11242-014-0430-4

Natural Convection Boundary Layer Flow over a Horizontal Plate Embedded in a Porous Medium Saturated with a Nanofluid: Case of Variable Thermophysical Properties

H. Zargartalebi · A. Noghrehabadi · M. Ghalambaz · Ioan Pop

Received: 15 May 2014 / Accepted: 27 November 2014 / Published online: 7 December 2014

Abstract There is a rising interest in application of nanofluids in porous media. As such, this paper is aimed at numerically investigating convective boundary layer flow over a plate embedded in a porous medium filled with nanofluid. Influence of multifarious boundary layers' applications namely concentration boundary layer of nanoparticles and thermal ones on thermal conductivity and dynamic viscosity of the nanofluid is studied. A new enhanced boundary condition, zero mass flux of nanoparticles through the surface, is adopted to calculate the volume fraction of nanoparticles on the surface. Furthermore, the effect of different practical non-dimensional parameters such as Brownian motion, thermophoresis, Lewis number, and buoyancy ratio on the hydrodynamic, thermal, and concentration boundary layers is investigated. It is revealed that an increase in buoyancy ratio culminates in temperature rise and velocity reduction. The results also show that as the dimensionless Lewis number increases, the fraction of nanoparticles at the sheet soars; on the other hand, the variation of Lewis number does not have considerable effect on the thermal and hydrodynamic boundary layers. Moreover, introducing an enhancement ratio as a criterion to examine the variation of thermal convective coefficient reveals that this value is a decreasing function of buoyancy ratio parameter. In some cases, the value of enhancement ratio becomes less than unity as the buoyancy ratio gets stronger.

Keywords Nanofluid · Porous medium · Boundary layer · Enhancement ratio

H. Zargartalebi · A. Noghrehabadi (✉)
Department of Mechanical Engineering, Shahid Chamran University of Ahvaz, Ahvaz, Iran
e-mail: a.r.noghrehabadi@gmail.com; noghrehabadi@scu.ac.ir

M. Ghalambaz
Department of Mechanical Engineering, Dezful Branch, Islamic Azad University, Dezful, Iran

I. Pop
Department of Mathematics, Babeş-Bolyai University, 400048 Cluj-Napoca, Romania

List of Symbols

D_B	Brownian diffusion coefficient (m^2/s)
D_T	Thermophoretic diffusion coefficient (m^2/s)
F	Rescaled nanoparticles volume fraction, nanoparticles concentration
g	Gravitational acceleration vector
h	Convective heat transfer coefficient (J/m^2)
k_{eff}	Effective thermal conductivity of the porous medium (W/m K)
K	Permeability of porous medium
Le	Lewis number
N_b	Brownian motion parameter
NC_f	Thermal conductivity concentration coefficient
NC_T	Thermal conductivity temperature coefficient
N_r	Buoyancy ratio
NV_f	Viscosity concentration coefficient
NV_T	Thermal viscosity coefficient
N_t	Thermophoresis parameter
p	Pressure (Pa)
Ra_x	Local Rayleigh number
S	Dimensionless stream function
T	temperature (K)
$\bar{u}$, $\bar{v}$	Darcy velocity components along x and y directions (m/s)
(x, y)	Cartesian coordinates

Greek Symbols

α	Thermal diffusivity (m^2/s)
β	Volumetric expansion coefficient of fluid
ε	Porosity
η	Dimensionless distance
θ	Dimensionless temperature
μ_{eff}	Viscosity of fluid (Pa s)
ν_{eff}	Cinematic viscosity
ρ	Density (kg/m^3)
ρ_c	Heat capacity (J/m^3 K)
τ	Parameter defined by Eq. (5)
φ	Dimensionless nanoparticles volume fraction
ψ	Stream function

Subscripts

∞	Free stream
m	Porous medium
bf	The base fluid
drift-flux	The drift flux model
nf	Nanofluid
p	Nanoparticles
w	Sheet, wall, surface

1 Introduction

Investigation of convective flow in porous media has been attracted a lot of attention recently. Due to enhanced physical and chemical properties, the nanofluids have found numerous applications in mechanical, civil, and chemical engineering. These applications subsume geothermal energy recovery, thermal energy storage, thermal insulation of building, underground dispose of nuclear and non-nuclear waste, and crude oil extraction. Nanofluids are engineered convective fluids that consist of nanoparticles or nanofibers, with conventional size of 1–100 nm, suspended in the fluid. A comprehensive review of the topic has been accomplished by Nield and Bejan (2013), Ingham and Pop (2005), and Vafai (2005, 2010).

The presence of nanoparticles or nanofibers in the host fluid would increase the thermal conductivity of the fluid, and consequently it is anticipated to improve convective heat transfer of nanofluid with respect to the base fluid.

Recent experiments on the thermophysical properties of nanofluids demonstrate that the presence of nanoparticles in the base fluid also impacts on other thermophysical properties such as dynamic viscosity, density, and heat capacity of the mixture. In addition, when nanofluid is subjected to temperature gradient, the thermophoresis force causes concentration gradient of nanoparticles in the base fluid (Buongiorno 2006). The previous studies (Bachok et al. 2010; Noghrehabadi et al. 2012; Yacob et al. 2011) showed that heat transfer boundary layer's characteristics of nanofluids alter due to slip velocity of nanoparticles as well as thermophysical properties. Accordingly, taking aforementioned facts into account, the heat transfer coefficient may increase or even decrease by dispersing nanoparticles in the base fluid.

Different aspects of nanofluids' convective boundary layer over flat plate have been investigated using Buongiorno (2006) model. For instance, Gorla and Chamkha (2011) analyzed the boundary layer flow and heat transfer of nanofluids over a horizontal plate embedded in a porous medium. They evaluated the quantities of practical interest such as friction factor and surface heat transfer rate. Aziz et al. (2012) have also studied steady boundary layer in free convection flow passes over a horizontal flat plate embedded in porous structure saturated with a water-based nanofluid containing gyrotactic microorganisms. Anjali Devi and Andrews (2011) have investigated an incompressible, viscous, forced convective laminar boundary layer flow of alumina water and copper water nanofluids over a plate. They found that suspending nanoparticles in the base fluid leads to heat transfer enhancement, and it becomes more appreciable as the nanoparticle's volume fraction increases. Khan and Pop (2010) have also studied boundary layer flow and heat transfer of nanofluids over a linear stretching sheet using the Buongiorno (2006) model. Noghrehabadi et al. (2012) have considered a partial slip velocity for the nanofluid at the sheet. They (Noghrehabadi et al. 2013) have also examined the effect of convective boundary condition below the sheet. Nield and Kuznetsov (2010a) have evaluated the natural convective heat transfer of nanofluid passes by a vertical plate using numerical solution.

In all of the aforementioned studies, it was assumed that the concentration of nanoparticles is actively controlled on the surface at a constant volume fraction of φ_w. However, it is not clear that how the volume fraction of nanoparticles on the surface could be actively controlled. In a very recent study conducted by Kuznetsov and Nield (2013), a new boundary condition for concentration of nanoparticles on the surface is proposed. They assumed that the surface of the wall is impermeable to the nanoparticles, and hence, the mass flux of nanoparticles through the surface is zero. Thus, the volume fraction of nanoparticles would be passively adjusted on the surface by the boundary layer. In practical terms, this new boundary condition is physically much more realistic than the fixed volume fraction of nanoparticles on the

surface. In other words, there is not any verification to have active control of nanoparticle volume fraction at the boundary.

Behseresht et al. (2014) have focused on the practical range of non-dimensional parameters of nanofluids and found that the Brownian motion and thermophoresis parameters were assumed very larger than their practical values in most of the previous studies. They concluded that the effect of the energy transport as a consequence of nanoparticles' migration in the natural convective flows is negligible; however, the concentration boundary layer of nanoparticles remains significant, and a significant boundary layer of nanoparticles could strongly affect the local values of thermal conductivity and dynamic viscosity of the mixture.

Accordingly, the effect of local volume fraction and temperature has not been taken into account, whereas the experimental observations and numerical investigations show that even very low volume fraction of nanoparticle and temperature variation can significantly affect the thermophysical properties of the nanofluid (Wang et al. 1999; Masuda et al. 1993; Koo and Kleinstreuer 2004; Chon et al. 2005). Khanafer and Vafai (2011) have accomplished a comprehensive study on variants of nanofluids' thermophysical properties. They have developed the effective thermal conductivity and dynamic viscosity correlations by evaluating the reported experimental data.

In the previous studies on boundary layer flow, heat and mass transfer, the effect of the local volume fraction of nanoparticles on the thermal conductivity and dynamic viscosity of the nanofluid was neglected. Zero nanoparticles' mass flux on the surface, practical range of nanofluid parameters, and considering the effect of nanoparticles boundary layer on the thermal conductivity and dynamic viscosity of nanofluids are the motivations for conducting the present new fundamental study on the natural convective boundary layer flow of nanofluids over a horizontal flat plate embedded in a saturated porous medium. As such, thermal conductivity and dynamic viscosity of nanofluid are considered a function of local volume fraction and temperature. Moreover, an enhancement ratio as a criterion to assess heat transfer improvement of nanofluid is proposed. In addition, inserting zero mass flux of nanoparticles on the surface, the volume fraction of nanoparticles on the surface is obtained and analyzed in details. Furthermore, the effect of non-dimensional parameters on the hydrodynamic, thermal, and concentration boundary layers, as well as the quantities of practical interest, reduced Nusselt number, and the enhancement ratio, are studied. We, therefore, believe that the present paper is original with very interesting new results on nanofluids.

2 Mathematical Model

A two-dimensional steady flow over a flat plate embedded in a porous medium is considered in the present study. There is local thermal equilibrium in the porous medium so that $T_f = T_p = T$, where T_f and T_p are the temperatures of fluid and of the solid phases, respectively. It is assumed that nanoparticles are suspended in the nanofluid using either surfactant or surface charge technology. This prevents nanoparticles from agglomeration and deposition on the porous matrix (Kuznetsov and Nield 2013; Nield and Kuznetsov 2009, 2010a, b). It is also worth mentioning that a macroscopic set of the governing equations for describing heat transfer in nanofluid saturated porous media was derived rigorously using a volume averaging theory, for possible heat transfer applications of metal foams filled with nanofluids as high performance heat exchangers and has been described in a very interesting recently published paper by Sakai et al. (2014).

Practically, the experimental results have shown that the nanoparticles could remain stable for about 3 weeks; therefore, stable suspension of the nanoparticles is a reasonable assump-

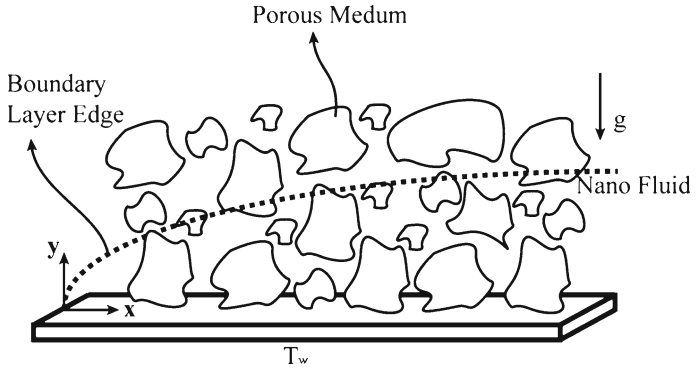

Fig. 1 Coordinate system and physical model

tion. The coordinate system is chosen such that the x-axis is aligned along the horizontal plate and the y-axis is normal to the plate. A schematic view of the physical model is shown in Fig. 1. Based on the scale analysis conducted by Buongiorno (2006), the nanoparticles in the fluid are swayed according to the Brownian and thermophoresis forces. The thermophoresis effect tends to propel the nanoparticles from hot point to cold one. Accordingly, in the present study, the hot plate makes nanoparticles to move away from the sheet. In contrast, the Brownian motion propels nanoparticles from a high concentration point to a low one. Therefore, the Brownian motion force tends to uniform nanoparticles concentration in the base fluid. Thus, because of the thermophoresis and Brownian motion effects, a concentration boundary layer of nanoparticles forms over the plate. As the nanofluids are a dilute mixture of base fluid and nanoparticles, the interaction between nanoparticles could be neglected (Buongiorno 2006). Further, it is important to explain how nanofluid flow is possible in a porous medium. It has been shown by Wu et al. (2010, 2011) that the porous matrix works as a filter for nanoparticles. This demonstrates that we are simulating here a real physics problem of natural convection boundary layer flow over a horizontal plate embedded in a porous medium saturated with a nanofluid using the mathematical nanofluid model proposed by Buongiorno (2006).

Considering that Oberbeck–Boussinesq approximation is valid, the governing equations comprising the continuity equation, momentum (Darcy) equation, thermal energy equation, and conservation for nanofluid are expressed as follows (Nield and Kuznetsov 2009, 2010b):

$$\frac{\partial \bar{u}}{\partial x} + \frac{\partial \bar{v}}{\partial y} = 0, \tag{1}$$

$$\frac{\mu_{\mathrm{eff,nf}}}{K}\bar{u} = -\frac{\partial \bar{p}}{\partial x}, \tag{2}$$

$$\frac{\mu_{\mathrm{eff,nf}}}{K}\bar{v} = -\frac{\partial \bar{p}}{\partial y} + \left[(1-\varphi_\infty)\,\rho_{\mathrm{f0}}\beta\left(\bar{T}-\bar{T}_\infty\right) - \left(\rho_{\mathrm{p}}-\rho_{\mathrm{f0}}\right)\left(\bar{\varphi}-\bar{\varphi}_\infty\right)\right] g. \tag{3}$$

Using cross-differentiation, one can eliminate the pressure p and obtain the ensuing equations

$$\frac{\partial \mu_{\mathrm{eff,nf}}}{\partial y}\frac{\bar{u}}{\mu_{\mathrm{eff,nf}}} + \frac{\partial \bar{u}}{\partial y} - \frac{\partial \mu_{\mathrm{eff,nf}}}{\partial x}\frac{\bar{v}}{\mu_{\mathrm{eff,nf}}} - \frac{\partial \bar{v}}{\partial x} = -\frac{(1-\bar{\varphi}_\infty)g\rho_{\mathrm{f0}}K\beta}{\mu_{\mathrm{eff,nf}}}\frac{\partial \bar{T}}{\partial x} + \frac{(\rho_{\mathrm{p}}-\rho_{\mathrm{f0}})gK}{\mu_{\mathrm{eff,nf}}}\frac{\partial \bar{\varphi}}{\partial x}, \tag{4}$$

$$\bar{u}\frac{\partial \bar{T}}{\partial x}+\bar{v}\frac{\partial \bar{T}}{\partial y}=\frac{1}{(\rho_{\mathrm{c}})_{\mathrm{nf}}}\left[\frac{\partial}{\partial x}\left(k_{\mathrm{eff,nf},\infty}\frac{\partial \bar{T}}{\partial x}\right)+\frac{\partial}{\partial y}\left(k_{\mathrm{eff,nf},\infty}\frac{\partial \bar{T}}{\partial y}\right)\right]$$
$$+\tau\left[D_{\mathrm{B}}\left(\frac{\partial \bar{\varphi}}{\partial x}\frac{\partial \bar{T}}{\partial x}+\frac{\partial \bar{\varphi}}{\partial y}\frac{\partial \bar{T}}{\partial y}\right)+\frac{D_{\mathrm{T}}}{T_{\infty}}\left[\left(\frac{\partial \bar{T}}{\partial x}\right)^{2}+\left(\frac{\partial \bar{T}}{\partial y}\right)^{2}\right]\right], \tag{5}$$

$$\bar{u}\frac{\partial \bar{\varphi}}{\partial x}+\bar{v}\frac{\partial \bar{\varphi}}{\partial y}=D_{\mathrm{B}}\left(\frac{\partial^{2}\bar{\varphi}}{\partial x^{2}}+\frac{\partial^{2}\bar{\varphi}}{\partial y^{2}}\right)+\frac{D_{\mathrm{T}}}{\bar{T}_{\infty}}\left(\frac{\partial^{2}\bar{T}}{\partial x^{2}}+\frac{\partial^{2}\bar{T}}{\partial y^{2}}\right), \tag{6}$$

subject to

$$\bar{v}=0,\quad \bar{T}=\bar{T}_{\mathrm{w}},\quad D_{\mathrm{B}}\frac{\partial \bar{\varphi}}{\partial y}+\frac{D_{\mathrm{T}}}{\bar{T}_{\infty}}\frac{\partial \bar{T}}{\partial y}=0\quad \text{at}\quad y=0,$$
$$\bar{u}\to 0,\quad \bar{T}\to \bar{T}_{\infty},\quad \bar{\varphi}\to \bar{\varphi}_{\infty}\quad \text{as}\quad y\to\infty. \tag{7}$$

Here, $\bar{u}$ and $\bar{v}$ represent the fluid filtration velocity component along x and y directions, respectively, $\bar{\varphi}$ is nanoparticle volume fraction, $k_{\mathrm{eff,nf}}$ is effective thermal conductivity of the nanofluid, $\tau=\varepsilon(\rho_{\mathrm{c}})_{\mathrm{p}}/(\rho_{\mathrm{c}})_{\mathrm{f}}$, and the physical meaning of other quantities is mentioned in the List of Symbols. Furthermore, the diffusion term at $y=0$ comprises two parts due to the existence of Brownian motion and thermophoresis effect. Therefore, in this boundary condition the last term should be considered in nanofluid flow simulation and could not be eliminated. It is worth mentioning that the zero mass flux of nanoparticles on the surface, i.e., $D_{\mathrm{B}}(\partial\bar{\phi}/\partial y)+D_{\mathrm{T}}/T_{\infty}(\partial T/\partial y)=0$, may result in the negative values of nanoparticle volume fraction on the surface when the thermophoresis effect is the dominant force with respect to Brownian motion. Accordingly, the zero volume fractions of nanoparticles on the surface would be a substitute for the boundary condition in such cases as the negative volume fraction of nanoparticles is not physically allowed.

Expressing following similar transportations, the governing partial equations could reduce to non-linear ordinary differential equations

$$\eta=\frac{y}{x}Ra_{\mathrm{nf,x}}^{\frac{1}{3}},\quad S=\frac{\psi}{\alpha_{\mathrm{m}}Ra_{\mathrm{nf,x}}^{\frac{1}{3}}},\quad \theta=\frac{\bar{T}-\bar{T}_{\infty}}{\bar{T}_{\mathrm{w}}-\bar{T}_{\infty}},\quad f=\frac{\bar{\varphi}-\bar{\varphi}_{\infty}}{\bar{\varphi}_{\infty}}, \tag{8}$$

where η denotes the similarity variable, Ra_x is Rayleigh number, α_{m} is the effective thermal diffusivity of the porous medium, and ψ is the stream function defined as $\bar{u}=\partial\psi/\partial y$ and $\bar{v}=-\partial\psi/\partial x$, which satisfies continuity equation. Substituting Eq. (8) into Eqs. (4)–(6), we obtain the following ordinary (similarity) differential equations:

$$\left(\frac{\mu_{\mathrm{eff,nf}}}{\mu_{\mathrm{eff,nf},\infty}}\right)S''+\left(\frac{\mu_{\mathrm{eff,nf}}}{\mu_{\mathrm{eff,nf},\infty}}\right)'S'=\frac{2}{3}\eta\left(\theta'-N_{\mathrm{r}}f'\right), \tag{9}$$

$$\left(\frac{k_{\mathrm{eff,nf}}(f,\,\theta)}{k_{\mathrm{eff,nf},\infty}}\right)\theta''+\frac{1}{3}S\theta'+\left(\frac{k_{\mathrm{eff,nf}}(f,\,\theta)}{k_{\mathrm{eff,nf},\infty}}\right)'\theta'+N_{\mathrm{b}}f'\theta'+N_{\mathrm{t}}\theta'^{2}=0, \tag{10}$$

$$f''+\frac{1}{3}LeSf'+\frac{N_{\mathrm{t}}}{N_{\mathrm{b}}}\theta''=0, \tag{11}$$

subject to

$$S(0)=0,\quad \theta(0)=1,$$
$$S'(\infty)\to 0,\quad \theta(\infty)\to 0,\quad f(\infty)\to 0. \tag{12}$$

Notice that the boundary condition for concentration is considered as

$$N_{\mathrm{b}}f'(0)+N_{\mathrm{t}}\theta'(0)=0. \tag{13}$$

As mentioned before, the zero mass flux of nanoparticles on the wall, i.e., Eq. (13) may lead to negative values of volume fraction of nanoparticles on the surface. In this case, this boundary condition would be replaced by the zero volume fraction of nanoparticles as follows:

$$f(0) = -1, \tag{14}$$

in which the dimensionless variables are considered as follows:

$$N_b = \frac{\tau D_B \bar{\phi}_\infty}{\alpha_{nf,\infty}}, \quad N_t = \frac{\tau D_T (T_w - T_\infty)}{\alpha_{nf,\infty} T_\infty}, \quad N_r = \frac{(\rho_p - \rho_{f0})\phi_\infty}{\rho_{f0}(1-\phi_\infty)\beta(T_w - T_\infty)},$$
$$Le = \frac{\nu_{eff,nf,\infty}}{D_B}, \quad \alpha_m = \frac{k_{eff,nf,\infty}}{(\rho_c)_{nf,\infty}}, \quad Ra = \frac{(1-\phi_\infty) g K \rho_{f0} \beta (T_w - T_\infty) x}{\mu_{eff,nf,\infty}\alpha_m}. \tag{15}$$

The physical parameter, namely the local Nusselt number Nu_x is defined as below.

$$Nu_x = \frac{h \cdot x}{k_{eff,nf,\infty}} = \frac{q_w x}{k_{eff,nf,\infty}(T_w - T_\infty)}, \tag{16}$$

where the surface heat flux q_w is introduced as

$$q_w = -k_{eff,nf,w}\left(\frac{\partial T}{\partial y}\right)_{y=0}. \tag{17}$$

Substituting Eq. (17) in Eq. (16) and using Eq. (8), the local Nusselt number is obtained as

$$Nu_x Ra_{nf,x}^{-\frac{1}{3}} = -\frac{k_{eff,nf,w}}{k_{eff,nf,\infty}}\theta'(0), \tag{18}$$

in which $N_r = Ra_{nf,x}^{1/3} Nu_x$ is the reduced Nusselt number.

Consider that the thermal conductivity and dynamic viscosity are approximated as function of temperature and concentration through the following equations:

$$\frac{k_{eff,nf}}{k_{eff,nf,\infty}} = 1 + NC_f \frac{\phi - \phi_\infty}{\phi_\infty} + NC_T \frac{T - T_\infty}{T_w - T_\infty}, \tag{19}$$

$$\frac{\mu_{eff,nf}}{\mu_{eff,nf,\infty}} = \frac{\exp\left(NV_f \frac{\phi - \phi_\infty}{\phi_\infty}\right)}{1 + NV_T \frac{T - T_\infty}{T_w - T_\infty}}. \tag{20}$$

Here, the coefficients NC_f, NC_T, NV_f, and NV_T stand for thermal conductivity concentration, thermal conductivity temperature, viscosity concentration, and thermal viscosity, respectively. In essence, the magnitudes of these coefficients depend on the nanofluid characteristics and also T_∞, T_w, and φ_∞.

3 Results and Discussion

Solving the above equations helps us with estimating various parameters explained in the following paragraphs. Figure 2 compares the thermal conductivity of nanofluid computed through Eq. (19) with that of Ethylene Glycol when $NC_f = 0.1627$ and $NC_T = 0.0738$. The values of NC_f and NC_T were obtained using accurate fitting on the experimental data.

This figure illustrates that the linear relation in Eq. (19) could truly approximate the thermal conductivity of the nanofluid as a function of the temperature and the concentration. Pastoriza-Gallego et al. (2014) measured the magnitude of dynamic viscosity of Ethylene Glycol–Zinc

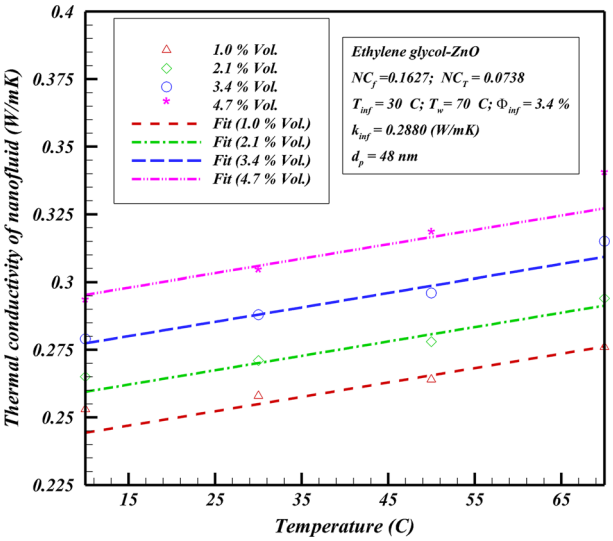

Fig. 2 A comparison between thermal conductivity of Eq. (19) and available experimental data (Pastoriza-Gallego et al. 2014)

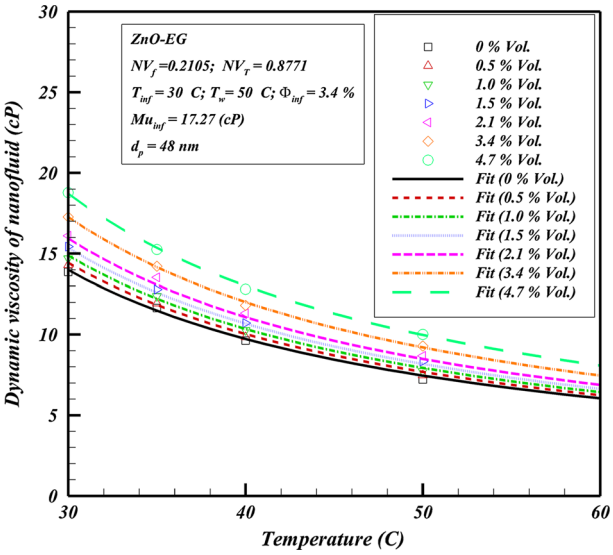

Fig. 3 A comparison of thermal conductivity between reported experimental data (Pastoriza-Gallego et al. 2014) and Eq. (23)

Oxide nanofluid in different temperature and concentration values. The nanoparticles were provided in the size of 48 and 4.6 nm. The nanofluid was dispersed under ultrasonic vibration for 16 min. The dynamic viscosities of nanofluid computed by Pastoriza-Gallego et al. (2014) are compared with Eq. (20) in Fig. 3.

Figure 3 shows that Eq. (20) could be used as an alternative to experiment.

In order to assess the variation of heat transfer of the nanofluid, an enhancement ratio is introduced as

$$\frac{h_{\text{drift-flux}}}{h_{\text{bf}}} = \frac{k_{\text{eff,nf,w}}\theta'_{\text{nf}}(0)\,Ra_{\text{nf,x}}^{1/3}}{k_{\text{eff,bf,w}}\theta'_{\text{bf}}(0)\,Ra_{\text{bf,x}}^{1/3}}. \tag{21}$$

The enhancement ratio is the ratio of the convective heat transfer of nanofluid to the convective heat transfer of the base fluid. The evaluations showed that the reduced Nusselt number could not estimate the enhancement of heat transfer because of the presence of nanoparticles in the base fluid. In fact, using nanoparticles in the base fluid alters the value of thermal conductivity, dynamic viscosity, and other thermophysical properties, and these changes render calculation of heat transfer intricate. As an illustration, the Rayleigh numbers of base fluid and nanofluid are not identical; accordingly, the heat transfer coefficient of nanofluid, h_{nf}, could even be less than h_{bf}. Thereupon, the variation of reduced Nusselt number could not meticulously detect the enhancements caused by the presence of nanoparticles in the base fluid. Despite the reduced Nusselt number, the alterations of both thermal conductivity and dynamic viscosity are considered in the enhancement ratio parameter ($h_{\text{drift-flux}}/h_{\text{bf}}$). In other words, since the enhancement ratio approximately subsumes all the crucial thermophysical properties, it could be feasibly applied to make a comparison between nanofluid and base fluid heat transfer.

Substituting Eqs. (19) and (20) in Eqs. (18) and (21) and using similar transportations [Eq. (8)], the reduced Nusselt number and enhancement ratio are calculated, respectively, as

$$Nu_{\text{r}} = Nu_x Ra_x^{-1/3} = -\left(1 + \text{NC}_\phi f(0) + \text{NC}_\text{T}\right)\theta'_{\text{nf}}(0), \tag{22}$$

$$\frac{h_{\text{drift-flux}}}{h_{\text{bf}}} = \left[(1 - \text{NC}_\text{f})\exp\left(-\text{NV}_\text{f}\right)\frac{(\rho_\text{c})_{\text{nf}}}{(\rho_\text{c})_{\text{bf}}}\right]^{1/3}\frac{1 + \text{NC}_\text{f} f(0) + \text{NC}_\text{T}}{1 - \text{NC}_\text{f} + \text{NC}_\text{T}}\frac{\theta'_{\text{nf}}(0)}{\theta'_{\text{bf}}(0)}. \tag{23}$$

The velocity, temperature, and concentration quantities are computed solving set of Eqs. (9)–(11) using relevant boundary conditions [Eqs. (12) and (13)]. Using finite difference method with adaptable size of mesh and the three-stage Lobatto III, a formula associated with a collocation formula to uniform the error in the domain of the solution, the set of Eqs. (9)–(11) are solved. The details of solution method can be found in Shampine et al. (2000). In this method, η_∞ is replaced with a large value of 10. In order to validate the numerical procedure, the values of $-\theta'(0)$ and $-f'(0)$ at selected magnitudes of N_r in the case which similarity solution for natural convection over an impermeable flat plate embedded in a porous medium saturated with a nanofluid is performed (Gorla and Chamkha 2011). It is worth noticing that the nanoparticle fraction at the surface is assumed to be constant and $N_\text{b} = 0.3$, $N_\text{t} = 0.1$, and $Le = 10$. Moreover, the thermal conductivity and dynamic viscosity of nanofluid are assumed to be constant. The comparison in Table 1 shows that the results are in good agreement with those results reported by the Gorla and Chamkha (2011) and Aziz et al. (2012). It is also clear that $\eta_\infty = 10$ is adequate for numerical computations, and hence, $\eta_\infty = 10$ is adopted for all calculations in the present study.

In order to study the effects of different parameters such as N_b, N_t, N_r, etc., on the boundary layer flow, heat and mass transfer, a practical range of this parameters has been considered. For water-based nanofluids which include nanoparticles of 100 nm diameters at room temperature, the Brownian diffusion coefficient D_B and the thermophoresis coefficient, D_T, are in the order of 10^{-11} (Buongiorno 2006). As a case in point, for water-based fluids filled with 100 nm Al_2O_3 nanoparticles, the values of D_B and D_T are evaluated as 4.3948×10^{-11} and 9.946×10^{-11},, respectively. The buoyancy ratio, N_r, is in the range of 0–9.7 $\times$

Table 1 Compare the values of $-\theta'(0)$ and $-f'(0)$ for natural convective boundary layer flow

N_r	Gorla and Chamkha (2011)		Aziz et al. (2012)		Present	
	$-\theta'(0)$	$-f'(0)$	$-\theta'(0)$	$-f'(0)$	$-\theta'(0)$	$-f'(0)$
0	0.32790	1.49867	–	–	0.32775	1.49726
0.1	0.32633	1.48416	0.32586	1.48225	0.32586	1.48224
0.2	0.32462	1.46816	0.32393	1.46686	0.32393	1.46686
0.3	0.32244	1.45266	0.32195	1.45106	0.32196	1.45107
0.4	0.32093	1.43639	0.31992	1.43482	0.31992	1.43482
0.5	0.31859	1.41950	–	–	0.31784	1.41811

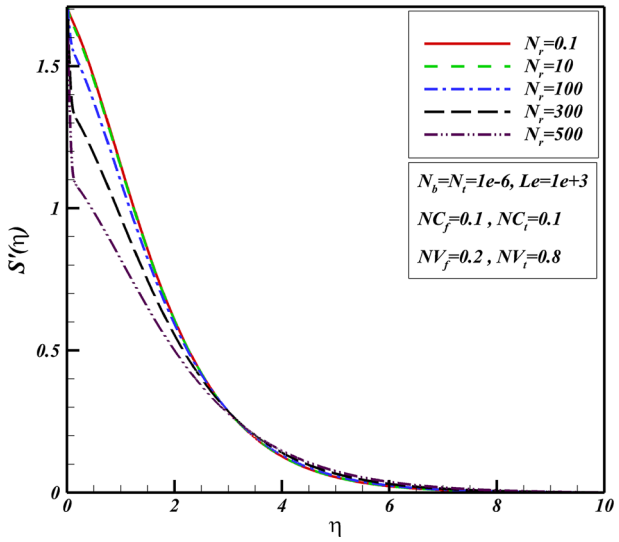

Fig. 4 The effect of buoyancy ratio on the velocity profile

10^{+3}, and the Lewis number is in the range of $1 \times 10^{+3}$ to $5 \times 10^{+5}$. Furthermore, it is found that the values of N_b and N_t are very small, ranging from 1×10^{-8} to 1×10^{-4}.

In order to survey the impact of buoyancy variation on the velocity and the temperature values, the velocity and the temperature profiles for different N_r quantities are depicted in Figs. 4 and 5. It is worth mentioning that variation of N_r does not have considerable effect on the dimensionless concentration profile.

Initial drastic decrease in velocity is noticeable in Fig. 4, i.e., $\eta < 3$, and afterward, the velocity gradient declines gradually as η increases. In other words, increase of the buoyancy ratio leads to velocity drop next to the surface. That is to say as N_r increases, the temperature and concentration values change; therefore, considering the dynamic viscosity correlation, i.e., Eq. (20), and also governing equations, i.e., Eqs. (9)–(11), it leads to drastic reduction in velocity.

Figure 5 shows that the non-dimensional temperature value increases due to augmentation of buoyancy ratio. In fact, since N_r is a ratio of ΔC to ΔT, as N_r increases, the mass transfer

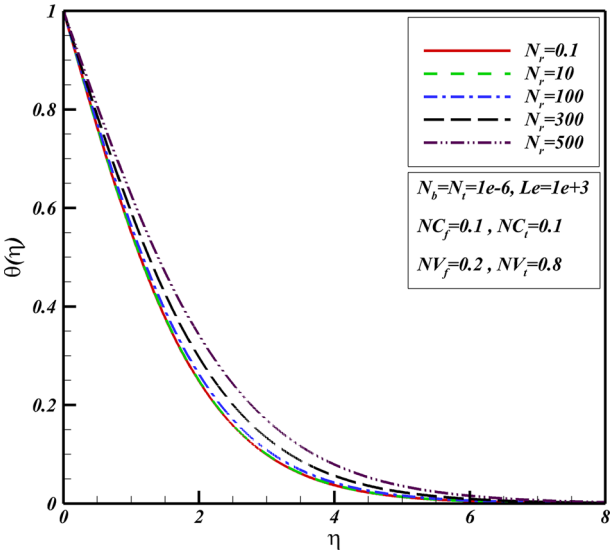

Fig. 5 Effect of N_r on the temperature profile

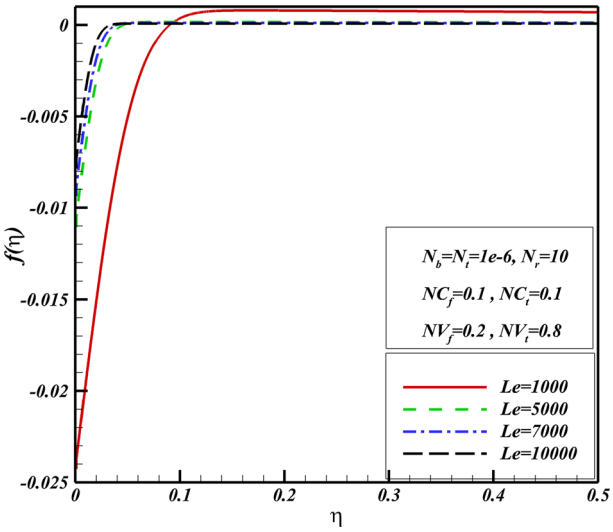

Fig. 6 Concentration profiles in different Lewis number

of nanoparticles becomes stronger than the heat transfer force. As a result, the temperature gradient drops down gradually as buoyancy ratio increases.

The effect of the Lewis number on the concentration boundary layer is shown in Fig. 6.

In accordance with Fig. 6, the nanoparticle fraction in vicinity of the sheet is lower than ambient volume fraction and the increase of Lewis number results in $f(0)$'s rise. In addition, an account of the fact that the Lewis number is a ratio of hydrodynamic boundary layer to concentration boundary layer and since the hydrodynamic boundary layer remains fixed in various Lewis numbers, as Lewis number increases, the thickness of the concentration

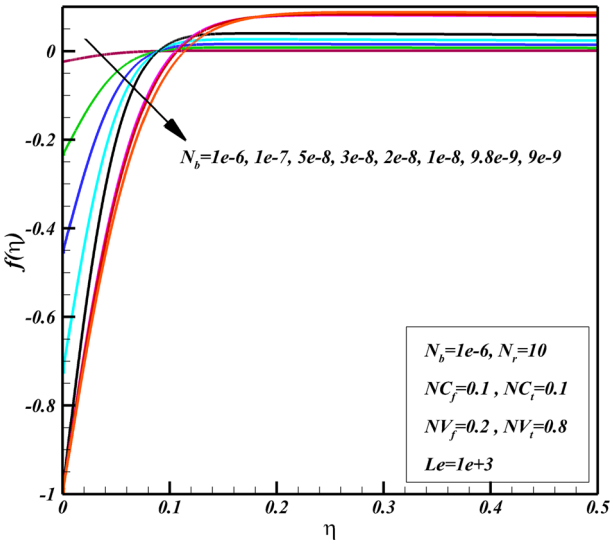

Fig. 7 Effect of N_b on non-dimensional volume fraction

boundary layer decreases. Furthermore, it is seen that in high values of the Lewis number the difference between concentration profiles diminishes. It is worth noticing that the thermal boundary layer is only weakly dependent on Lewis number as well as hydrodynamic boundary layer.

The effect of Brownian motion and thermophoresis parameters on the concentration profile are depicted in Figs. 7 and 8.

Figure 7 represents that the value of non-dimensional concentration at the sheet depends on the magnitude of N_b and alters significantly. Comparing the parameters N_b and N_t, it is found that as N_b decreases, the value of $f(0)$ drops as well. Practically, decrease of N_b leads to the Brownian effect's decline and consequently fraction of nanoparticles decreases. As it is seen, the concentration profiles are categorized in two branches. The first one consists of the profiles which initiate from -1, i.e., the volume fraction at the sheet becomes less than zero (which was fixed as zero), and the second consists of the profiles where $f(0) > -1$ or $\varphi > 0$. Conversely, it is observed that the nanoparticle fractions of the first group are higher than the second one in the computational domain.

In accordance with Fig. 8, as N_t diminishes, the non-dimensional volume fraction at the sheet decreases. Moreover, the thickness of concentration boundary layer becomes small as the thermophoresis parameter decreases. As an illustration, when $N_\mathrm{t} = 5 \times 10^{-9}$, the thickness of the concentration boundary layer becomes comparatively trivial.

In Figs. 6, 7 and 8 the concentration profiles are depicted for $0 < \eta_\infty < 0.5$ to clearly show the behavior of these profiles; however, it should be noticed the numerical calculations were performed for $\eta_\infty = 10$.

The effect of Brownian motion parameter on the velocity and temperature profiles is presented in Figs. 9 and 10.

Figure 9 depicts that the values of velocity next to the surface increase as N_b goes up. In addition, it is seen that the hydrodynamic profile declines noticeably adjacent to the surface in the low values of Brownian motion parameter, e.g., $N_\mathrm{b} = 2 \times 10^{-8}$. The drastic changes are because of noticeable variation in concentration next to the surface. Nonetheless, the thickness

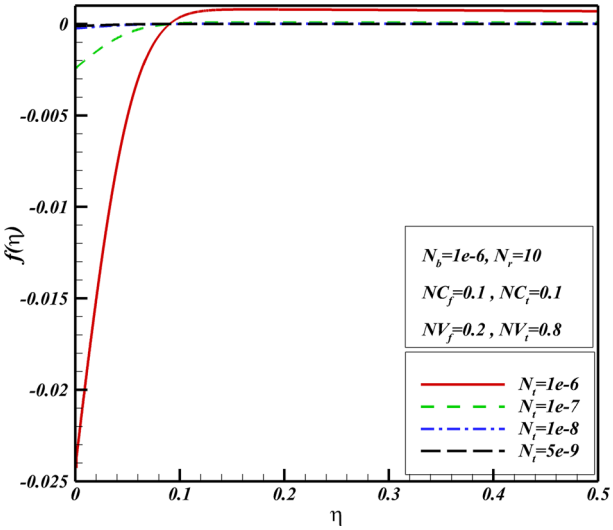

Fig. 8 Effect of N_{t} on the non-dimensional concentration profile

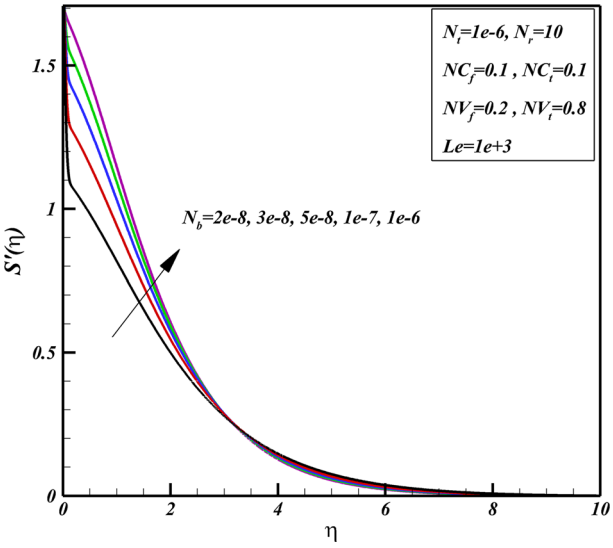

Fig. 9 Effect of N_{b} on the hydrodynamic boundary layer

of hydrodynamic boundary layer remains constant in various values of N_{b}. In essence, the buoyancy force is constructed from two parts. The first part is because of the temperature and volumetric expansion of the fluid, and the second part is because of the migration of nanoparticles, i.e., nanoparticles mass transfer. As seen in Fig. 9, there is a thin layer of nanoparticles over the plate. In this region, i.e., $0 < \eta < 0.4$, the migration of nanoparticles because of the thermophoresis force is strong. When the buoyancy ratio is about the moderate value of 10, i.e., $N_{\mathrm{r}} = 10$, the buoyancy force because of mass transfer of nanoparticles is the dominant force in this thin region. However, beyond the mentioned region, i.e., $\eta > 0.4$,

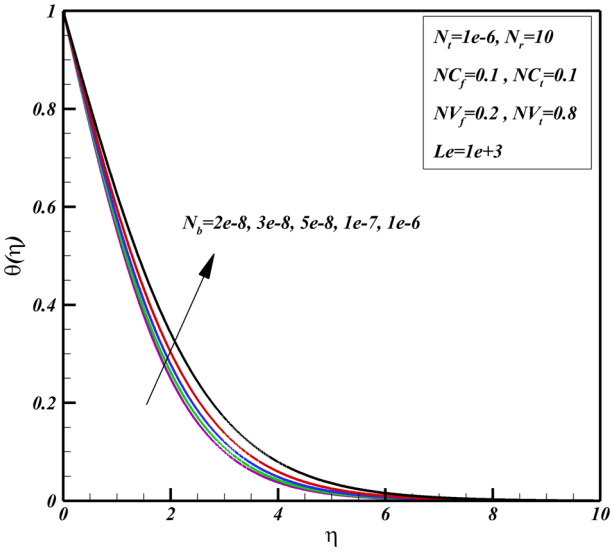

Fig. 10 Effect of N_b on the thermal boundary layer

the buoyancy force because of the mass transfer of nanoparticles diminishes and the volume expansion one becomes the dominant force. Therefore, it can be concluded that the behavior of velocity profiles in the vicinity of the plate is the result of concentration boundary layer of nanoparticles. Hence, in order to understand the behavior of velocity profiles in Fig. 9, we need to follow the behavior of concentration profiles in Fig. 7. As seen in Fig. 7, as N_b decreases the volume fraction of nanoparticles on the surface decreases. This is because of the fact that the Brownian motion is the force which tends to uniform the nanoparticles in the boundary layer. Any decrease of the Brownian motion parameter, i.e., N_b, means that the Brownian force is weakened and in contrast the thermophoresis force can sweep more particles away from the hot plate. The decrease of volume fraction of nanoparticles directly increases the buoyancy force because of the mass transfer of nanoparticles. Therefore, as seen in Fig. 9, the decrease of the Brownian motion parameter, i.e., N_b, increases the velocity profiles in the region in which the boundary layer of nanoparticles is effective, $0 < \eta < 0.4$. Far from the plate, i.e., $4 < \eta < 8$, the effect of buoyancy force because of the migration of nanoparticles completely diminishes, and hence, the velocity profiles are almost coincident.

As it is seen, the temperature values augment as the Brownian motion parameter goes up. In other words, when the value of N_b is low, the temperature gradient increases. As a result, the thickness of the thermal boundary layer becomes small. In fact, as N_b decreases the effective thermal diffusivity of the porous medium, i.e., α_m, would intensify and consequently it leads to increase in temperature gradient.

Proceeding with the analysis, we investigate the effect of N_b, N_t, N_r, and Le on the reduced Nusselt number and the enhancement ratio, respectively (Figs. 11, 12, 13, 14).

Figures 11 and 12 indicate that the reduced Nusselt number diminishes as the value of N_r goes up. Furthermore, the augmentation of Lewis number leads to increase in the value of Nu_r. When the parametric value of N_b increases or the value of N_t decreases, the slope of Nu_r variation declines. As the buoyancy ratio soars, the difference between Nu_r values is more pronounced.

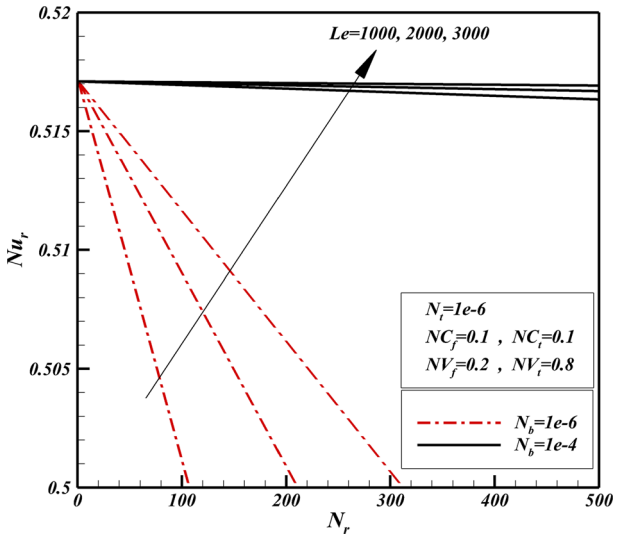

Fig. 11 Effect of N_{b}, N_{r}, and Le on the reduced Nusselt number

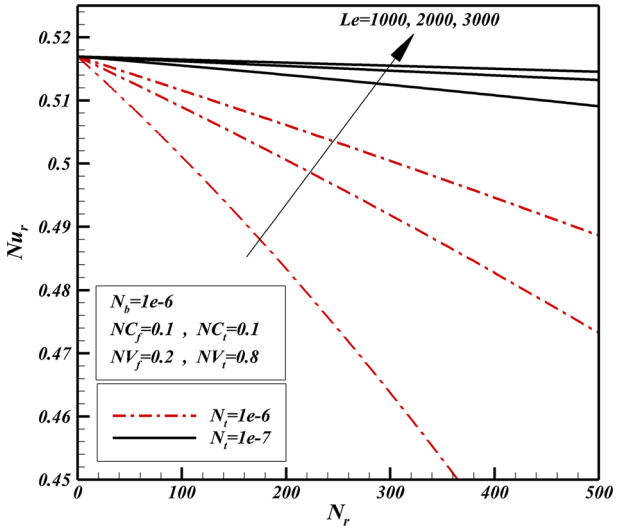

Fig. 12 Effect of N_{t}, N_{r}, and Le on the reduced Nusselt number

According to Figs. 13 and 14, as N_{r} increases, the value of enhancement ratio decreases. Depending on the parametric values of N_{b}, N_{t}, and dimensionless Lewis number, the value of $h_{\mathrm{nf}}/h_{\mathrm{bf}}$ becomes different. As the Lewis number increases, the value of enhancement ratio increases as well. On the other hand, in spite of N_{b}, decrease of N_{t} leads to increase in the $h_{\mathrm{nf}}/h_{\mathrm{bf}}$ magnitude. It is also interesting to note that the enhancement ratio could be less than unity in high values of N_{r}.

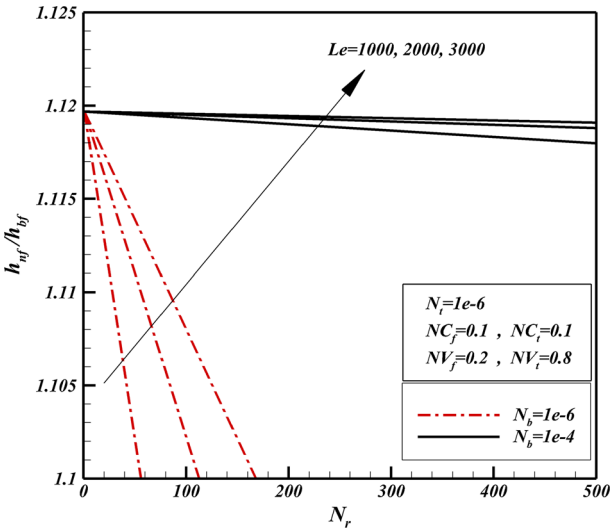

Fig. 13 Effect of N_b, N_r, and Le on the enhancement ratio

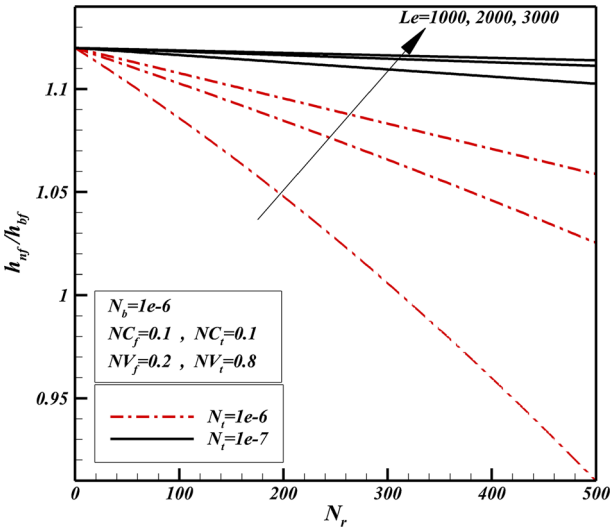

Fig. 14 Effect of N_t, N_r, and Le on the enhancement ratio

4 Conclusion

The boundary layer flow over a flat plate embedded in a porous medium filled with nanofluid is studied. It is assumed that the flow is laminar, the sheet is impermeable, and the mass flux of nanoparticles on the sheet is zero. The influences of the quantities of practical interest such as N_b, N_t, N_r, and Le on the hydrodynamic, thermal, and concentration boundary layer is evaluated. Here is a summary of the main results:

(1) As the buoyancy ratio increases, the temperature and the velocity magnitudes increase and decrease, respectively. In addition, the concentration boundary layer is relatively

insensitive to changes in N_r. Furthermore, a scrutiny of the effect of N_b on the thermal and hydrodynamic boundary layer depicts that increase in the Brownian motion leads to increase in temperature and velocity values.

(2) As the dimensionless Lewis number increases, the fraction of nanoparticles at the sheet goes up as well. In the range of high Lewis numbers, the variation of this parameter rarely affects the concentration boundary layer. Moreover, the results reveal that the Lewis number does not have noticeable impact on the temperature and velocity profiles.

(3) As the Brownian motion parameter (N_b) decreases, the nanoparticles tend to move away from the sheet.

(4) The reduced Nusselt number and the enhancement ratio are diminished as the buoyancy ratio increases. The augmentation of the Lewis number and the Brownian motion and decrease in the thermophoresis parameter comparably give rise to Nu_r and h_{nf}/h_{bf}. In addition, the results show that the enhancement ratio may be less than unity in range of high buoyancy ratio.

Acknowledgments The authors would like to thank the very competent Reviewers for the valuable comments and suggestions. The first author is grateful to Shahid Chamran University of Ahvaz for its support. Noghrehabadi, Zargartalebi and Ghalambaz acknowledge the Iran Nanotechnology Initiative Council (INIC) for financial support.

References

Anjali Devi, S.P., Andrews, J.: Laminar boundary layer flow of nanofluid over a flat plate. Int. J. Appl. Math. Mech. **7**, 52–71 (2011)

Aziz, A., Khan, W.A., Pop, I.: Free convection boundary layer flow past a horizontal flat plate embedded in porous medium filled by nanofluid containing gyrotactic microorganisms. Int. J. Therm. Sci. **56**, 48–57 (2012)

Bachok, N., Ishak, A., Pop, I.: Boundary-layer flow of nanofluids over a moving surface in a flowing fluid. Int. J. Therm. Sci. **49**, 1663–1668 (2010)

Behseresht, A., Noghrehabadi, A., Ghalambaz, M.: Natural-convection heat and mass transfer from a vertical cone in porous media filled with nanofluids using the practical ranges of nanofluids thermo-physical properties. Chem. Eng. Res. Des. **92**, 447–452 (2014)

Buongiorno, J.: Convective transport in nanofluids. ASME J. Heat Transf. **128**, 240–245 (2006)

Chon, C.H., Kihm, K.D., Lee, S.P., Choi, S.U.S.: Empirical correlation finding the role of temperature and particle size for nanofluid (Al_2O_3) thermal conductivity enhancement. Appl. Phys. Lett. **87**, 153107 (2005)

Gorla, R.S.R., Chamkha, A.: Natural convective boundary layer flow over a horizontal plate embedded in a porous medium saturated with a nanofluid. J. Mod. Phys. **2**, 62–71 (2011)

Ingham, D.B., Pop, I.: Transport Phenomena in Porous Media III. Elsevier, Oxford (2005)

Khan, W.A., Pop, I.: Boundary-layer flow of a nanofluid past a stretching sheet. Int. J. Heat Mass Transf. **53**, 2477–2483 (2010)

Khanafer, K., Vafai, K.: A critical synthesis of thermophysical characteristics of nanofluids. Int. J. Heat Mass Transf. **54**, 4410–4428 (2011)

Koo, J., Kleinstreuer, C.: A new thermal conductivity model for nanofluids. J. Nanopart. Res. **6**, 577–588 (2004)

Kuznetsov, A.V., Nield, D.A.: The Cheng–Minkowycz problem for natural convective boundary layer flow in a porous medium saturated by a nanofluid: a revised model. Int. J. Heat Mass Transf. **65**, 682–685 (2013)

Masuda, H., Ebata, A., Teramae, K., Hishinuma, N.: Alteration of thermal conductivity and viscosity of liquid by dispersing ultra-fine particles (dispersion of c-Al_2O_3, SiO_2 and TiO_2 ultra-fine particles). Netsu Bussei **4**, 227–233 (1993)

Nield, D.A., Bejan, A.: Convection in Porous Media, 4th edn. Springer, New York (2013)

Nield, D.A., Kuznetsov, A.V.: Thermal instability in a porous medium layer saturated by a nanofluid. Int. J. Heat Mass Transf. **52**, 5796–5801 (2009)

Nield, D.A., Kuznetsov, A.V.: Natural convective boundary-layer flow of a nanofluid past a vertical plate. Int. J. Therm. Sci. **49**, 243–247 (2010a)

Nield, D.A., Kuznetsov, A.V.: The onset of convection in a horizontal nanofluid layer of finite depth. Eur. J. Mech. B **29**, 217–223 (2010b)

Noghrehabadi, N., Pourrajab, R., Ghalambaz, M.: Effect of partial slip boundary condition on the flow and heat transfer of nanofluids past stretching sheet prescribed constant wall temperature. Int. J. Therm. Sci. **54**, 253–261 (2012)

Noghrehabadi, A., Pourrajab, R., Ghalambaz, M.: Flow and heat transfer of nanofluids over stretching sheet taking into account partial slip and thermal convective boundary conditions. Heat Mass Transf. **49**, 1357–1366 (2013)

Pastoriza-Gallego, M.J., Lugo, L., Cabaleiro, D., Legido, J.L., Piñeiro, M.M.: Thermophysical profile of ethylene glycol-based ZnO nanofluids. J. Chem. Thermodyn. **73**, 23–30 (2014)

Sakai, F., Li, W., Nakayama, A.: A rigorous derivation and its applications of volume averaged transport equations for heat transfer in nanofluid saturated metal foams. In: Proceedings of the 15th International Heat Transfer Conference, IHTC-15, Kyoto, Japan, 10–15 August 2014

Shampine, L.F., Kierzenka, J., Reichelt, M.W.: Solving boundary value problems for ordinary differential equations in MATLAB with bvp4c. Tutorial notes (2000)

Vafai, K.: Handbook of Porous Media, 2nd edn. Taylor and Francis, New York (2005)

Vafai, K.: Porous Media: Applications in Biological Systems and Biotechnology. CRC Press, Boca Raton (2010)

Wang, X., Xu, X., Choi, S.U.S.: Thermal conductivity of nanoparticles–fluid mixture. J. Thermophys. Heat Transf. **13**, 474–480 (1999)

Wu, M., Kuznetsov, A.V., Jasper, W.J.: Modeling of particle trajectories in an electrostatically charged channel. Phys. Fluids **22**, 043301 (2010)

Wu, G., Kuznetsov, A.V., Jasper, W.J.: Distribution characteristics of exhaust gases and soot particles in a wall-flow ceramics filter. J. Aerosol Sci. **42**, 447–461 (2011)

Yacob, N.A., Ishak, A., Nazar, R., Pop, I.: Falkner–Skan problem for a static and moving wedge with prescribed surface heat flux in a nanofluid. Int. Commun. Heat Mass **38**, 149–153 (2011)